Research article

Iron-loaded *Punica granatum* peel: An effective biosorbent for the excision of arsenite from water

Bishnu Datt Pant [a,1], Sangita Adhikari [a,1], Nabina Shrestha [a], Janaki Baral [a], Hari Paudyal [b], Kedar Nath Ghimire [b], Megh Raj Pokhrel [b], Bhoj Raj Poudel [a,*]

[a] *Department of Chemistry, Tri-Chandra Multiple Campus, Tribhuvan University, Kathmandu, 44600, Nepal*
[b] *Central Department of Chemistry, Tribhuvan University, Kathmandu, 44618, Nepal*

A B S T R A C T

The occurrence of arsenic in the surroundings raises apprehension because its detrimental impacts on both human health and the ecology. Since adsorption is an effective, affordable method that can be adjusted to specific environmental circumstances, it is a sustainable solution for the removal of arsenic from the aquatic environment. Utilizing biomass that has been chemically activated may be a viable way to increase the adsorption capacity of the material, reduce arsenic pollution, and protect the environment and human health. In the proposed research, Fe(III) loaded saponified *Punica granatum* peel (Fe(III)-SPGP) has been synthesized to remove arsenic from aqueous solutions. FTIR and SEM analysis were utilized to carry out the characterization of the biosorbents. Batch experiments were carried out by altering several factors including pH and contact time, in addition to initial concentration and desorption. The most effective pH for As(III) adsorption using Fe(III)-SPGP was discovered to be 9.0. After determining that a pseudo-second-order kinetic model was the one that provided the greatest fit for the results of the experiment, the model developed by Langmuir was applied. It was discovered that the maximum adsorption of As (III) that could be adsorbed by Fe(III)-SPGP was 63.29 mg/g. The spent biosorbent may easily be reused again in subsequent applications. Based on these findings, Fe(III)-SPGP shows promise as a cheap effective sorbent for excising contaminants of As(III).

1. Introduction

All life on Earth is dependent on water, as it is the most abundant component on the planet. Human activity is a major contributor to the degradation of water quality, which has emerged as a significant environmental issue in today's global society. Additionally, it is believed that the biggest obstacle to achieving the sustainable development goals by 2030 is water scarcity [1]. Heavy metals are particularly worrisome as a class of contaminants since they are extremely poisonous, do not degrade, and remain relatively constant over time [2]. Damage to biological macro-molecules is mostly caused by oxidation when heavy metals bind to DNA and nuclear proteins. Heavy metals also contribute to cellular dysfunction [3]. The main hazardous heavy metal contaminants include arsenic (As), nickel (Ni), mercury (Hg), cobalt (Co), cadmium (Cd), and chromium (Cr) among others [4,5]. The pollution caused by these heavy metals is not only harmful to the environment; it also poses a significant threat to human health. Arsenic is among the potentially

---

harmful heavy metals that is being investigated as a serious water toxin which can have a variety of consequences on people's health. Arsenic is a potentially harmful non-essential component of natural environment, may give rise issues with skin, nervous and circulatory systems, as well as cancer and even death in extreme cases [6,7]. Arsenic can be generated through naturally occurrences including erosion actions, biologic processes, and eruption of volcanos, along with manmade actions including the refining of petroleum, the mining of gold, and the application of herbicides and insecticides in agriculture [8,9]. Arsenic can exist in oxidation states ranging from −3, 0, +3 and + 5, with As(III) and As(V) being main types of element that are hazardous and present in water [10]. The World Health Organization (WHO) has determined that the highest amount of arsenic that can be present in drinking water is 10 μg/L [3].

It is believed that arsenic can cause both cancer and mutations in living organisms. There are a variety of heavy elements, each of which, when exposed to their environment, produces a toxic and hazardous byproduct. In addition to these, arsenic is extremely poisonous and distinct from the others; it can be found in soil and water as the inorganic species arsenate. Furthermore, it can be found in groundwater and seawater as arsenite, along with various other metals such as copper, lead, and iron. An exposure to arsenic through the mouth or the digestive tract can cause immediate as well as persistent symptoms in the environment. Arsenic has been connected to causing striking hurdles in a bodily organ system, including the respiratory, nervous, circulatory, hematological, immunological, endocrine, hepatic, renal, and reproductive system and development, as well as epigenetic modification and genetic abnormalities [11].

Because of the consequence of the arsenic contamination, investigators have concentrated on a variety of aspects to find effective methods for detoxifying water. These techniques include adsorption, reversible osmosis, ion exchange, coagulation, nanofiltration, biological methods, membrane distillation, and photocatalytic oxidation, among others [12]. While there are various physical and chemical methods available for removing heavy metals, adsorption is notably productive and economical. The adsorption technique is environmentally safe and has a high removal capacity due to its selectivity and low formation of hazardous byproducts. Agricultural wastes have been the subject of recent studies because they are inexpensive, plentiful and include a number of polymeric compounds that can bind heavy metals effectively [13]. The process of adsorption is an immensely beneficial method, and through its utilization, the residual substances derived from agricultural waste, including fruit peels, shells, straw, sawdust, orange peels, and litchi pericarp, can be effectively employed for the elimination of metal toxicity [14]. Pomegranate peel based biosorbent is one example which is efficient, cheap, and a renewable resource for the ejection of hazardous heavy metals from the groundwater [15,16]. One of the popular fruit crops, pomegranate (*Punica granatum*) is grown in several nations, including Nepal. Pomegranate peel, which is a residual product of the fruit juice sector, is a less researched material with promising capabilities as a sorbent for the ejection of deleterious contaminants in aquatics bodies. Pomegranate peels, denoted as PP, may constitute up to 30 % of the overall weight of the fruit. Despite this fact, they are frequently discarded as residual waste and are easily obtainable at no cost or for a very low price [17]. In conjunction with lignin, sugar molecules, hemicellulose, cellulose, limonene, and other substances, it comprises around 10–15 % pectic substance [18]. Thus, modifying the biological polymer found in PP material to create a natural anion exchange for removing arsenic ions offers a novel and efficient solution in terms of financial and ecological issues. The triumph of this research lies in its creation of a eco-friendly material and reduction of farm waste. Therefore, the aim of this particular study is to utilize discarded pomegranate peel to develop a natural material for exchanging anions, capable of capturing arsenic oxyanions.

The pectic acid of pomegranate, when combined with calcium in saponified Punica granatum peel (SPGP), acts as a cation exchanger. This process aids in the uptake of metal ions through an exchange of cations reaction involving Ca(II) ion. Nevertheless, the process of biosorption of anionic species onto SPGP poses challenges, requiring further modifications to enhance its capacity as a biosorbent for anionic species. As a result, iron in its Fe(III) form was incorporated into the structure of SPGP to create locations for exchanging anions, which would then capture oxyanion arsenic. In our previous study, we investigated the potential of Zr(IV)-loaded pomegranate peel as an efficient bio-adsorbent for arsenic removal [19]. Past studies have highlighted zirconium as a highly effective metal for this application [3]. Nonetheless, the high cost associated with zirconium continues to be a significant barrier to its widespread use. Iron, which has a similar chemistry to zirconium, has demonstrated significant effectiveness in arsenic adsorption. Ferric hydroxide and ferric oxide are particularly noted for their strong selectivity toward arsenic [20–22]. By creating an adsorbent from pectin-rich pomegranate peel combined with the relatively inexpensive $FeCl_3$ salts, both the adsorption efficiency and the cost-effectiveness of the adsorbent can be substantially reduced. In the context of species containing oxygen donors such as oxyanions of arsenic, the Fe(III) cation demonstrates a robust electrostatic and coordinative attraction. Furthermore, modest Fe (III) ion concentrations do not harm human health. Under such conditions, Fe(III) has been chosen to modify previously proposed adsorbent, pomegranate peels in order to improve As(III) adsorption performance.

As far as we are aware, there are not any reports in the literature on adsorptive removal of As (III) using iron loaded pomegranate peel. This has led to the investigation using Fe(III) loaded pomegranate peel as a new material that can remove As(III) from water. As a result of the absence of a suitable economic material for arsenic removal, our study focused on developing inexpensive adsorbents using pomegranate. The financial feasibility is crucial for effectively absorbing arsenic from water in rural areas. The peel of the pomegranate, found abundantly as organic waste in many places, is distinguished by a range of functional groups on the surface. Additionally, it does not leach harmful substances into the water being treated, making it a key focus of our research efforts. Hence, the utilization of Fe(III)-SPGP is suggested as an innovative sorbent for the elimination of As(III) from the aqueous solution. These peels contain a wealth of nutrients and have a variety of medical applications in addition to their usage in the elimination of heavy metals [23,24]. FTIR, SEM, and EDS were among the characterization methods that were utilized to understand biosorbents. Various factors such as the pH of the solution, the duration of interaction, the amount of biosorbent used, and the concentration of As(III) were examined to understand their impacts, followed by a thorough analysis of the findings. The desorption study entailed the evaluation of the potential regeneration and reutilization of the biosorbent.

2. Materials and methods

2.1. Chemicals

Solely high-grade analytical chemical reagents were employed in the study, without undergoing any further purification procedures. The initial step involved the dissolution of a stock solution containing 1000 mg/L of arsenic trioxide (As_2O_3) in a solution comprising of 20 mL of 10M NaOH. Subsequently, the aforementioned solution was neutralized using nitric acid and subsequently diluted to obtain a final volume of 1000 mL. During the experiment, the stock solutions were subjected to many dilutions, which were carried out with double-distilled water.

2.2. Biosorbent preparation

Punica granatum (Pomegranate) fruit was gathered from a variety of locations across Bhotahity, including Indra Chowk and Bagbazar Fruit Shop Kathmandu, Bagmati Province, Nepal. After that, the peels of the pomegranate fruit were peeled, washed, and dried in the sunlight for a period of two to three days. After that, the dried peels were sliced into tiny pieces so that they could be ground in the laboratory mill. To obtain a fine and definite particle size, the fine powder made from pomegranate peels was passed through a filter with a mesh size of 150-μm. Next, it was placed in a clean, airtight container for storage. Because of the process by which the powdered pomegranate was obtained, it was first categorized as raw pomegranate peel (RPP). The method for preparing the Fe(III)-loaded saponified pomegranate peel was adapted from that described by Paudyal et al. [25]. Initially, a precise amount of 20 g of RPP was carefully measured out before being combined with 500 mL of saturated calcium hydroxide and agitated in a mechanical shaker. Following a 24-h saponification reaction between lime water and RPP ester groups, it was filtered and washed thoroughly for several rounds of decanting using distilled water to achieve a neutral pH. Then after, it was heated at 60 °C for 24 h and finally saponified pomegranate peels (SPGP) were collected as the product. To produce an anion exchange site for arsenite, Fe(III) was added into the polymer matrix of SPGP peel by loading. For this, 10 g of SPGP and 500 mL of 0.1 M $FeCl_3.6H_2O$ were stirred in a shaker for 24 h. The resultant product underwent filtering and distilled water washing to achieve a pH of neutrality. After being washed, the powder was put into an oven to dry. As a result of the aforementioned loading reaction, Fe(III) was loaded onto the SPGP by replacing calcium by iron, and the resulting material is designated as iron loaded SPGP which abbreviated as Fe(III)-SPGP hereafter. Scheme 1 depicts the chemical reactions that take place during the production of Fe(III)-SPGP. Iron generally forms the octahedral complex in aqueous solution, thus there is the possibility of binding six ligand around the iron's coordination sphere. Due to the expansive polymeric composition of pomegranate pectin, it is unfeasible for the chains of carboxylic acids in pomegranate peel to neutralize all charges of Fe (III) during the loading reaction. Hence, a few positive charges of Fe(III) are removed by the carboxylic acid groups found in pomegranate peel, while the remaining charges are balanced out by hydroxyl ions in a watery environment. Additional coordination numbers are fulfilled by water molecules. These hydroxyl and water ligands are inferred to be the major active center for arsenic adsorption.

2.3. Biosorbents characterization

The biosorbent surface's functional groups were identified using Fourier transform infrared spectroscopy (FTIR). The surface microstructure and other morphological behavior were imaged using scanning electron microscopy (SEM). To unveil the elemental makeup, the X-ray Energy Dispersive Spectrometer (EDS) was employed.

2.4. Biosorption experiments

The biosorption experiment of As(III) using Fe(III)-SPGP was done using a batch approach. To accomplish this task, a specific volume of a solution containing As(III) along with a known initial concentration and a certain amount of biosorbent were combined in a 100 mL flask and subjected to equilibration. To verify that the biosorbent and metal solution had reached equilibrium, the combination was shaken in a shaker at 298K for 12 h at a speed of 150 revolutions per minute. After the solution had equilibrated, it was filtered, and the filtrates from that process were used for a study of the remaining level of arsenic ions.
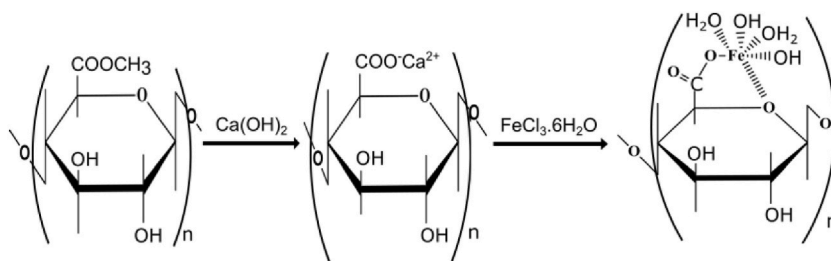
Scheme 1. Fe(III)-SPGP synthetic method utilizing saponification and Fe(III) loading.

The initial and equilibrium concentrations of As(III) in water samples were measured using an Inductively Coupled Plasma – Optical Emission Spectrometer (PerkinElmer Avio 220Max, ICP-OES). The calibration solutions were made using ICP standards for As (Sigma-Aldrich, 1000 ppm). pH, contact time, and initial metal ion concentrations at room temperature, to gather equilibrium data. During research involving batch adsorption, the effects of varying factors such as pH of the solutions, initial concentration of As(III) ion, influence of co-existing ions, and contact time were investigated. All experiments were performed in triplicate, and the results for As(III) analysis are presented as mean values $\pm$ standard error. Equations (1) and (2) were used to determine the equilibrium adsorption capacity, given by the symbol q_e (mg/g), and the percent of removing, denoted by the symbol Re% [26].

$$q_e = \frac{(C_o - C_e)V}{m} \tag{1}$$

$$R_e \% = \frac{(C_o - C_e)}{C_o} \times 100 \tag{2}$$

where, C_o represents the initial concentration in milligrams per liter, C_e represents the equilibrium time concentration of As(III) in milligrams per liter, m represents the biosorbent's mass in grams, and V is the solution's volume (L).

2.5. Modelling of experimental data

The process of monolayer adsorption on the surface of a biosorbent is characterized by the application of the Langmuir isotherm model. This model can be mathematically represented in two different forms: non-linearly with the utilization of Eq. (3) and linearly by means of Eq. (4) as outlined below [27],

$$q_e = \frac{q_{max.K_L.} C_e}{1 + K_L.C_e} \tag{3}$$

$$\frac{C_e}{q_e} = \frac{1}{q_{max} K_L} + \frac{C_e}{q_{max}} \tag{4}$$

where, K_L represents the Langmuir constant, which is expressed in milliliters per milligram, while q_{max} signifies the maximum adsorption capacity, denoted in milligrams per gram.

The separation factor, or dimensionless constant (R_L), is typically employed with Eq. (5) to evaluate the quality of a Langmuir isotherm. There are four possible outcomes for the adsorption process: $(0 < R_L < 1)$, unfavorable ($R_L > 1$), linear ($R_L = 1$) or Irreversible ($R_L = 0$).

$$R_L = \frac{1}{1 + (K_L C_O)} \tag{5}$$

With the help of non-linear Eq. (6) and linear Eq. (7), we can formulate the model for multiple layers adsorption on an uneven surface, which is specified by the Freundlich equation [28],

$$q_e = K_F (C_e)^{1/n} \tag{6}$$

$$\log q_e = \log K_F + \left(\frac{1}{n}\right) \log C_e \tag{7}$$

where, K_F [(mg g^{-1}) (L mg^{-1})$^{1/n}$] is Freundlich constant and n is Freundlich exponent.

By utilizing pseudo-first-order and pseudo-second-order models, the study investigated the adsorption kinetics of As(III) on the biosorbent. Eq. (8) is the standard form for the pseudo first order linear equation [25],

$$\log(q_e - q_t) = \log q_e - \frac{k1}{2.303} t \tag{8}$$

in which q_t (mg/g) represents the sorption capacity at time t, while k_1 (mg/g.min) denotes the rate constant for pseudo first order kinetics. In Eq. (9), we get an expression for a linear equation of pseudo second order,

$$\frac{t}{qt} = \frac{1}{k_2 q_e^2} + \frac{t}{qe} t \tag{9}$$

In the context of a pseudo second-order model, the rate constant is denoted as K_2 (g mg^{-1} min^{-1}).

By adding three different concentrations of each coexisting ions into a 25 mg/L arsenite solution, it was possible to assess the effects of competitive ions found in natural water on the biosorption of As(III). A similar procedure was used to prepare a blank sample without the use of a coexisting anion. The solution's pH was maintained at 9.0. After adding the 1 g/L dose of biosorbent, the sample was agitated for 12 h at the ambient temperature. To analyze the As(III) content, the filtrate were collected.

2.6. Desorption and regeneration test

When determining whether it is economically feasible, one of the most important considerations to take into account is how the biosorbent may be regenerated. It was determined that the biosorbent could be reused by following the processes that were disclosed [29]. The objective of this endeavor was to achieve an economic improvement in the adsorption process by replenishing and recycling the material. 0.1 M NaOH solution (stripping solution) was mixed with 25 mg of the spent biosorbent for 12 h to liberate the As(III) ion in order to evaluate the regeneration of Fe(III)-SPGP. Later on, it was filtered and dried. As(III) biosorption was again accomplished using the recovered biosorbent. To assess the reuse ability of the biosorbent, four successive cycles of the biosorption/regeneration process were conducted in equilibrium circumstances. For each succeeding cycle, the % biosorption of As(III) was assessed.

3. Results and discussion

3.1. Biosorbent characterization

The functional groups on the material were identified with the help of an important analytical technique called FTIR [30]. In the region of 4000-400 cm^{-1}, FTIR spectra of both unmodified raw RPP and chemically modified Fe(III)-SPGP were studied (Fig. 1). Biosorbents FTIR analysis can unveil the functional groups responsible for binding metal ions by comparing infra-red spectra prior to and subsequent to adsorption under ideal conditions. The noteworthy peak detected at 3340 cm^{-1} in feed material, RPP, originates from the elongated vibration of hydroxyl groups exist in pectin, hemicellulose, lignin and cellulose. The peak observed at a wavenumber of 2920 cm^{-1} can be attributed to the vibrational stretching of C-H bonds. Similarly, the peak detected at 1731 cm^{-1} is a result of the stretching vibrations of carboxylic acid and ester groups present in the biopolymer extracted from pomegranate peel. Following the process of saponification, the peak observed at 1731 cm^{-1} in SPGP vanishes as a result of the creation of the - O - Ca linkage within Ca - pectate. Simultaneously, a distinct peak emerges at 1420 cm^{-1}. The peak of the SPGP, originally at 1420 cm^{-1}, moved to a lower wave number (1410 cm^{-1}) after Fe(III) loading, as a result of the development of the - O - Fe linkage of Fe(III) - pectate in Fe (III)-SPGP. From this observation, it is declared that the easter and carboxylic functional groups has the main role for the saponification and iron loading, respectively.

Fig. 2 shows the SEM images of RPP, Fe(III)-SPGP, and the Fe(III)-SPGP adsorbed with As(III). The RPP surface was found to appear smooth and homogeneous, with few pores and voids (Fig. 2(a)). The presence of a waxy and dense layer was noted on the exterior of RPP, possibly attributed to the presence of sugars, pigments and some water soluble organic and inorganic compounds. After Fe(III) loading (Fig. 2(b)), the surface of the adsorbent became rough, and heterogeneous that contained numerous pores and voids. It provides evidence that the new material with different surface morphology has been formed. Surfaces became rough and porous as a result of chemical alteration, maybe due to the elimination of smooth and waxy components like glue, sugar molecules and limonene [31]. In case of As(III) adsorbed Fe(III)-SPGP (Fig. 2(c)), the surface roughness was found to be reduced. All the outcomes indicate that Fe(III) can be loaded onto RPP, which effectively adsorbed As(III) ions, which will be further proved by analyzing elemental composition of arsenic adsorbed Fe(III)-SPGP.

To determine elemental composition, the EDS spectrum of arsenic adsorbed Fe(III)-SPGP was recorded together with the mapping of individual elements as shown in Fig. S1 provided in the Supplementary Information (SI). The electronic layer imaging and its total elemental mapping is shown in Figure Fig. S1(a), which shows the existence of carbon, oxygen, iron, and arsenic as major elements. Further confirmation and comfort for visual observation were made by individual elemental mapping as shown in Fig. S1(b). This analysis further substantiated the presence of the specific elements, where green, gray, yellow and purple color indicates carbon, oxygen, arsenic and iron, respectively. For further confirmation, the EDS spectra of As-Fe(III)-SPGP was recorded as illustrated in Fig. S1(c). The analysis revealed that the elements such as carbon (65.29 %), oxygen (31.63 %), iron (2.09 %) and arsenic (0.99 %) were identified as the primary elements present in As-Fe(III)-SPGP, with binding energy values of 0.27, 0.54, 6.40, and 1.24 keV,
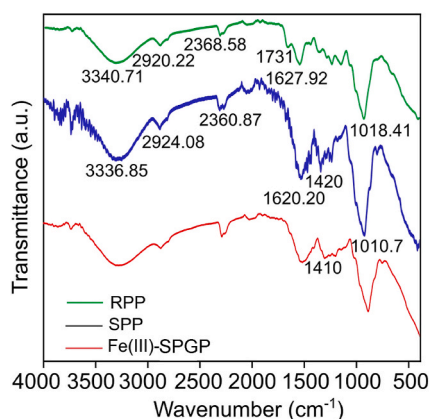

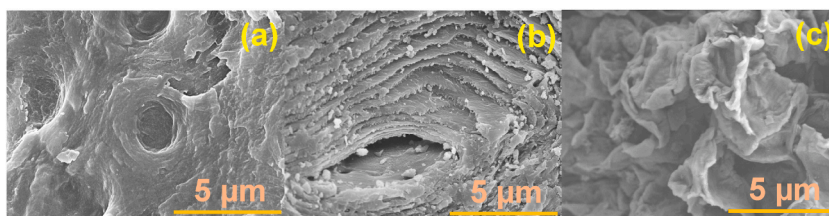**Fig. 1.** Ftir spectra of RPP, SPGP and Fe(III)-SPGP.

Fig. 2. SEM images of **(a)** RPP, (b) Fe(III)-SPGP prior to adsorption, and **(c)** Fe(III)-SPGP following the adsorption of As (III).

respectively. The observation of 0.99 % of arsenic in the sample of As-Fe(III)-SPGP provides the direct evidence that the Fe(III)-SPGP has significantly adsorbed arsenic ions.

3.2. Effect of solution pH

The impact of the pH level of the solution plays a crucial role in the realm of adsorption. Because of this, the biosorbent's surface charge, ionization level, and arsenic specification are all altered. This results in a shift not just in the degree of ionization and specification of arsenic but also in the outer charge of the biosorbent itself. The pH can determine whether the active site on the sorbent becomes protonated or deprotonated. The amount of As(III) that was adsorbed by a substance corresponds to the pH level of the solution. Fig. S2 provided in the SI illustrates the speciation of As(III) at various pH values [3].

For the biosorbents RPP and Fe(III)-SPGP, the maximum amount of As(III) was adsorbed at a pH of 9.0 (Fig. S3 provided in the SI). Arsenite primarily exists as neutral H_3AsO_3 in acidic conditions (pH < 7) and as $H_2AsO_3^-$ in basic conditions (pH 8–12). The speciation of arsenite affects its interaction with adsorbents, and the efficiency of the adsorbent can vary depending on the chemical form of the As(III) ion in solution. From a pH of 6.0–9.0, a higher percentage of adsorption was seen; after the pH rose above 9.0, the percentage of adsorption dropped off substantially. he abrupt drop in arsenite adsorption seen at high pH values (>10.0) may be related to the competitiveness between hydroxide ions and arsenite anions for the available adsorption sites [32]. Comparing the percentages of removal achieved by the two biosorbents, it is evident that Fe(III)-SPGP is significantly better, with a value of 76.7 % compared to RPP's 26.01 %. The adsorption process of Fe(III) leads to the development of additional anion exchange locations on the Fe(III)-SPGP surface, which contributes to the enhanced adsorption capacity of arsenite. Since RPP was not effective for As(III) adsorption, thus Fe (III)-SPGP is only the system for which we performed the further analysis at optimum pH 9.0.

3.3. Changes in As(III) adsorption on Fe(III)-SPGP as a function of contact time

By altering the contact period and keeping all additional variables constant, the biosorption of arsenite ions on Fe(III)-SPGP was examined and the result is shown in Fig. S4 provided in the SI. The findings indicate that the adsorption rate of As(III) was rapid initially, then gradually decreased before reaching equilibrium. The rapid adsorption at the beginning is attributed to the presence of a substantial quantity of active adsorption sites. As the lapse of time, some of the adsorption sites were occupied by arsenite anion so that a smaller number of biosorption sites are available for further adsorption leading to decrease of adsorption rate. After the occupation of all the adsorption sites by arsenite anion, there was no or negligible possibility of biosorption resulting adsorption equilibrium. The biosorption equilibrium was achieved at 90-min time at optimum pH of 9.
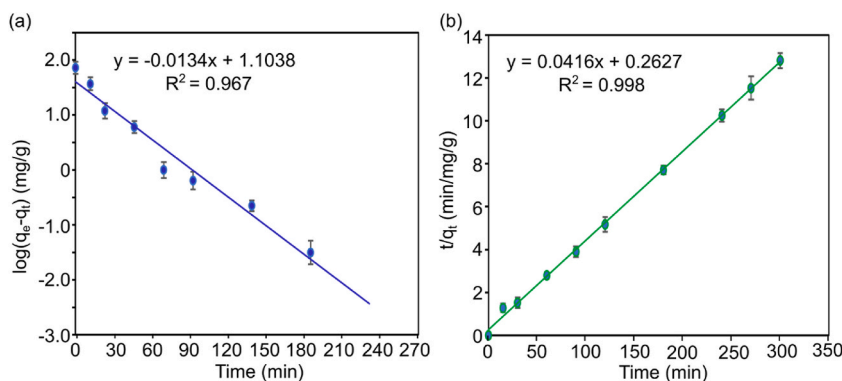

Fig. 3. Adsorption kinetics of As (III) on Fe(III)-SPGP: **(a)** PFO kinetic plot and **(b)** PSO kinetic plot. Values are presented as mean ± standard error (n = 3).

3.4. Biosorption kinetics studies

The properties and mechanism of the adsorption of As (III) onto Fe(III)-SPGP were investigated by using pseudo-first-order (PFO) and pseudo-second-order (PSO) kinetic models. Adsorption kinetics investigations were conducted at an optimal pH of 9. Two separate graphs of $\log(q_e-q_t)$ vs time (Fig. 3(a)) and t/q_t vs time (Fig. 3(b)) were plotted to evaluate the kinetics parameters of both models. The kinetic plot for As (III) adsorption showed that the measurement of correlation coefficients (R^2) for PSO was found to be greater (close to 1) than that of PFO. The kinetic parameter estimates are presented in Table 1.

The adsorption of As(III) onto Fe(III)-SPGP was effectively elucidated by the pseudo-second order kinetic model. It has been suggested that the ligand sites of exchange in Fe(III)-SPGP and the As(III) anion may contribute to the biosorption process through electron sharing or transfer. Evidence from prior investigations also suggested that As(III) biosorption favors a pseudo-second-order model [28,29].

3.5. Effect of initial concentration and isotherm modelling

When utilizing 25 mg of Fe(III)-SPGP at the most suitable pH settings, an analysis was carried out to assess the impact of varied initial concentrations of As(III) ranging between 10 and 500 mg/L, as illustrated in Fig. S5 provided in the SI. As per the results, an increase in the concentration of As(III) ions led to a rapid rise in biosorption capacity, followed by a gradual increase when it reached saturation (plateau) at high concentrations. One possible explanation for the initially high biosorption rate is that an increasing number of accessible sorption sites have been made available by the biosorbent. Once a certain concentration threshold is reached, not more biosorption can take place since no more sites are accessible. The removal of arsenic occurred more rapidly at lower concentrations in comparison to higher concentrations, implying that Fe(III)-SPGP is much more suitable for treating aqueous solutions containing very small quantities of arsenite.

Applying a variety of models to the data, such as the Langmuir (Fig. 4 (a)) and Freundlich (Fig. 4 (b)) isotherms, allowed the biosorption system to be determined through the process of fitting the data. When learning more about the properties of a biosorbent's surface, an adsorption isotherm is an invaluable tool. It offers a comprehensive explanation of the equilibrium ratio of metal ions, encompassing both the solid and liquid states, as well as the relationship between the metal ion and the biosorbent. The best fitting model for As(III) adsorption on Fe(III)-SPGP was identified using the results of the plots. Fig. 4(a) and **Figure (b)** show the Langmuir and Freundlich isotherms, respectively, that have been linearized for Fe(III)-SPGP, and a table contains the isotherm parameters that were calculated (Table 2). According to the isotherm analysis, the R^2 measurement of Fe(III)-SPGP for the Langmuir isotherm plot was 0.999, which is higher than the R^2 value 0.898 for the Freundlich isotherm. The Langmuir isotherm model was employed for the computation of the maximum adsorption capacity (qmax), resulting in a value of 63.29 mg/g, closely resembling the experimental measurement of 61.48 mg/g. The findings showed that adsorption on a single layer occurred, and that the biosorbent's active sites were evenly dispersed over its surface.

Further utilizing the Langmuir isotherm equation, it was discovered that the R_L values for As(III) on Fe(III)-SPGP between 0 and 1 as shown in Fig. 4 (c). This value is situated within the interval of ($0 < R_L < 1$), indicating the appropriateness of the process for the adsorption of As(III) and the compatibility of the adsorption data with the Langmuir adsorption isotherm [33].

Using Fe(III)-SPGP as an example, this study compares the maximum capacity for As(III) adsorption to that for various biomass-based biosorbents described in the literature (Table 3). According to the findings, the As(III) absorption capability of Fe(III)-SPGP is impressive when compared to the other biosorbents that have been reported. This finding suggests that Fe(III)-SPGP could be a promising contender for removing As(III) ions from water samples.

3.6. Influence of co-existing ions

It was determined how different competing ions affected the biosorption of As(III), and the outcomes are revealed in Fig. S6 provided in the SI. As can be observed in the figure, the presence of SO_4^{2-} and Cl^- at any concentration level, very marginally lowers the percentage of As(III) that is adsorbed when compared to the blank. This could be since these ions are less capable of binding than As (III) ions. However, the addition of PO_4^{3-} considerably decreased As(III) biosorption because phosphate and arsenite ions vie for binding sites on the biosorbent. Because of their identical chemical and structural properties in aqueous solutions, phosphate and arsenite cause a sharp decrease in arsenate biosorption [40].

3.7. Desorption study and reusability of Fe(III)-SPGP

The adsorbed metals should be removed from the biosorbent for the study of desorption before being regenerated for a subsequent cycle of the process. One way to effectively minimize costs is by employing a technique called biosorbent regeneration. Since As(III) ion

Table 1
As(III) adsorption kinetic parameters on Fe(III)-SPGP.

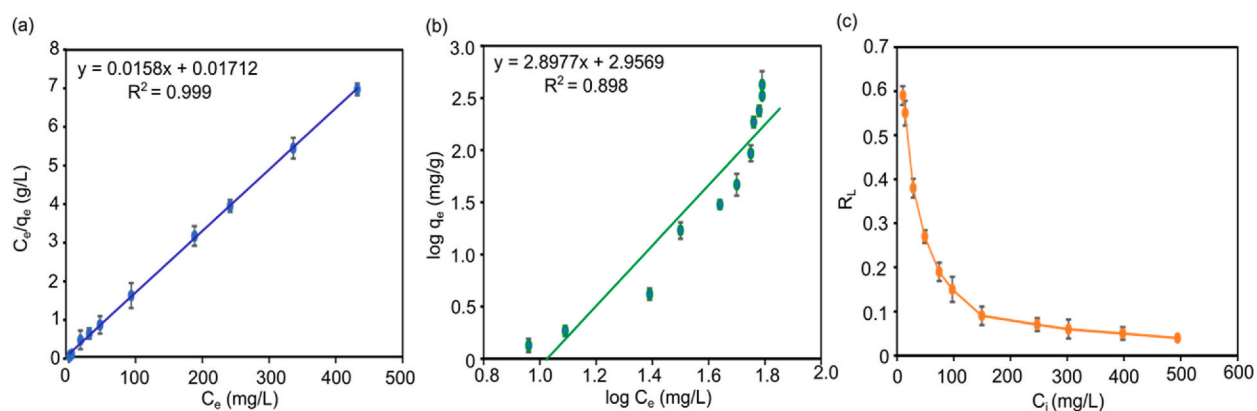| Kinetics models	Adsorbate	q_e(exp) (mg/g)	q_e(cal) (mg/g)	K_1 (min^{-1})	K_2 (mg/g/min)	R^2
PFO	As(III)	23.41	12.70	3.08×10^{-2}	–	0.967-
PSO	As(III)	23.41	24.03	–	6.60×10^{-3}	0.998

Fig. 4. Biosorption of As(III) onto Fe(III)-SPGP: **(a)** Langmuir isotherm, **(b)** Freundlich isotherm, and **(c)** change of R_L with initial As(III) concentration. Values are presented as mean $\pm$ standard error (n = 3).

Table 2
Adsorption of As(III) onto Fe(III)-SPGP: Isotherm parameters.

| Adsorbate	Langmuir Isotherm			Freundlich Isotherm		
	q_{max} (mg/g)	K_L (L/mg)	R^2	K_F [(mg g^{-1}) (L mg^{-1})$^{1/n}$]	$1/n$	R^2
As(III)	63.29	0.90	0.999	11.88	0.309	0.898

Table 3
Capacity for As(III) biosorption of different biosorbents compared to that of Fe(III)-SPGP.

Biosorbents	Optimal pH	q_m (mg/g)	Reference
Zr(IV)-loaded saponified pomegranate peel	8.0	72.52	[19]
La(III)-loaded saponified watermelon rind	12.08	37.73	[31]
Zr(IV)-loaded apple peels	9.0	15.68	[32]
Modified hazelnut shell	9.0	11.84	[34]
Zr-chitosan modified sodium alginate composite	–	43.19	[35]
Powdered almond shell	7.2	4.6	[36]
Iron-coated seaweeds	7.0	4.2	[37]
ZrO$_2$-coated sawdust	7.0	29.0	[38]
La$_2$O$_3$-coated sawdust	7.0	22.0	[38]
Iron dopped amino-functionalized sawdust	7.0	10.1	[39]
Fe(III)-SPGP	9.0	63.29	Present work

is weakly adsorbed on Fe(III)-SPGP at pH greater than 11, using an alkali solution makes it simple to desorb As(III) from the exhausted biosorbent. Therefore, the Fe(III)-SPGP which adsorbed As(III) can undergo rejuvenation for the purpose of reutilization by means of the application of a 0.1 M NaOH solution. The presence of a significant amount of OH$^-$ ions in the alkaline solution could have facilitated the exchange of adsorbed As(III) anions through a ligand exchange process [31]. The Fe(III)SPGP desorbed by NaOH was isolated and neutralized for reuse by rinsing with DI water. After desorption, up to four series of biosorption/desorption were conducted in order to assess the potential for reusing the biosorbent. The As(III) biosorption capacity declined from 76.6 % to 51.3 % after four consecutive cycles, as illustrated in Fig. S7. It was discovered that few attractive sites cannot be fully reversed through the desorption process. Even though its biosorption capacity decreased with repeated recycling, the Fe(III)SPGP was a greatly ecological and favorable biosorbent for removing As(III) from water solution. The desorption of As(V) from As(V) adsorbed Zr(IV) loaded saponified pomegranate peel [19]; Fe(III) loaded saponified pomelo peel [41] and desorption of Cr(VI) from Cr(VI) adsorbed modified *Lichi chinesis* seed powder [42], were seen in a manner resembling this.

3.8. Mechanism of As(III) adsorption and desorption on Fe(III)-SPGP

Scheme 2 depicts the process of adsorption and desorption of As(III) on Fe(III)-SPGP. The dominant monoanionic species (H$_2$AsO$_3^-$) and neutral species (H$_3$AsO$_3$) are considered to be accountable for replacing hydroxyl ions or water molecules during the adsorption of As(III). The process of surface protonation gives the biosorbent a positive charge. Electrostatic attraction phenomena occur between the protonated surface of the biosorbent and the monoanionic species (H$_2$AsO$_3$), leading to the adsorption of H$_2$AsO$_3$ onto the surface of Fe(III)-SPGP. It's possible that As(III) is adsorbed onto protonated sites of -OH in the Fe(III)-SPGP occurs via an ion-exchange
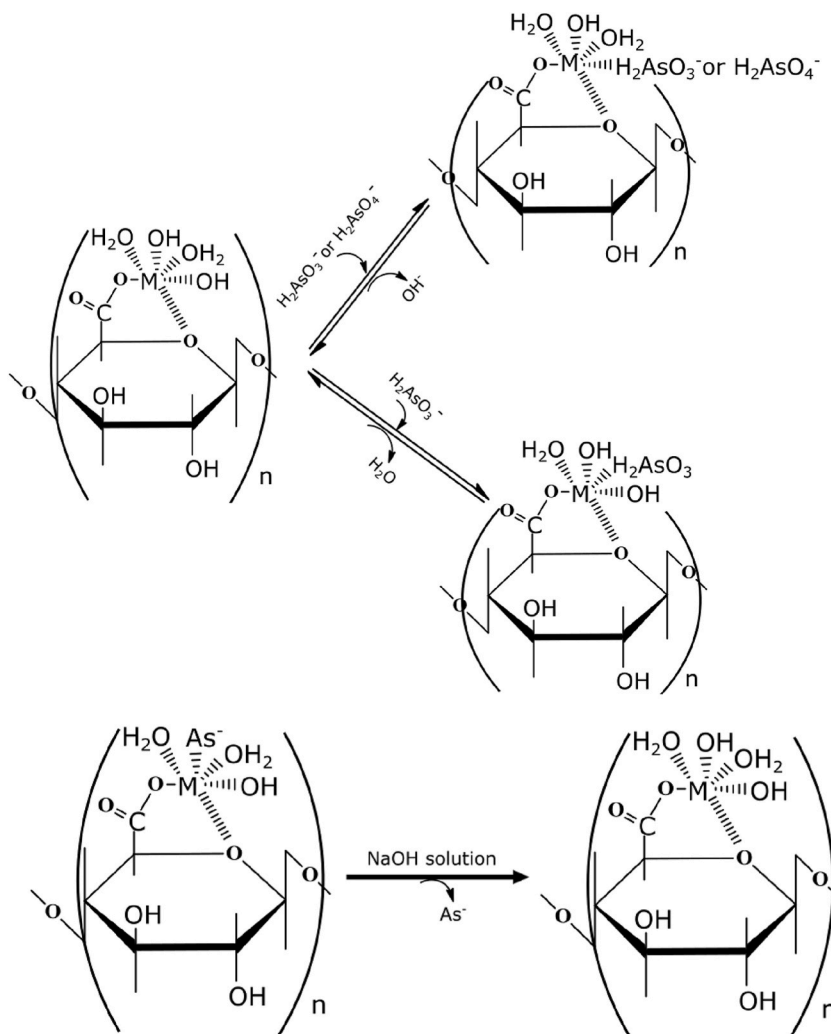
Scheme 2. Mechanism of As(III) adsorption and desorption on Fe(III)-SPGP.

process. Another possible mechanism for As(III) adsorption onto protonated sites of -OH inside the Fe(III)-SPGP involves an ion-exchange reaction [28,29]. The kinetic data for As(III) adsorption onto Fe(III)-SPGP align closely with the pseudo-second-order kinetic model, indicating that the process may be influenced by chemisorption. The results suggest that the adsorption of As(III) on the Fe (III)-SPGP surface is controlled by both ligand exchange, which forms inner-sphere surface complexes, and the electrostatic interactions between the negatively charged arsenate ions and the positively charged adsorbent's surface.

The biosorbent that has been used up by the biosorbent can be regenerated with the help of a NaOH solution, which also allows the As(III) ions to be recovered. In accordance with Scheme 1, the hydroxyl ions that are present in solution participate in a ligand replacement process with the sorbed oxyanions of As(III).

4. Conclusions

The elimination of As(III) by Punica granatum and its chemically modified form was investigated in this work, and their efficacy was evaluated by modulating a number of various factors. According to the findings of the investigation, it was determined that the Fe (III)-SPGP demonstrates effective potential in removing As(III) from water solutions through the process of adsorption. A variety of analytical methods, including FTIR, SEM, and EDS, were utilized to successfully characterize sorbents. The efficiency of the biosorbent was determined using a batch method with a number of parameters, including the pH of the solution, the length of time the biosorbent was in contact with the sample, and the amount of biosorbent used. It was discovered that Fe(III)-SPGP have a maximum adsorption capacity (q_{max}) of 63.29 mg/g. It has been determined that the Langmuir model was the one that is more appropriate, and that the pseudo-second-order kinetic model can adequately describe how the adsorption process works. This study reveals that an easy treatment procedure can be used to modify the pomegranate peel, which can be obtained at a low cost from readily available material. The current study was carried out using the batch method, however it is also possible to carry it out using the column method.

Furthermore, Fe(III)-SPGP exhibits promising characteristics as a biosorbent that can effectively eliminate toxic As(III) from industrial effluents.

Funding statement

Data availability statement

Data will be made available on request.

CRediT authorship contribution statement

Bishnu Datt Pant: Writing – review & editing, Conceptualization. **Sangita Adhikari:** Writing – review & editing. **Nabina Shrestha:** Writing – review & editing. **Janaki Baral:** Writing – review & editing, Formal analysis, Data curation. **Hari Paudyal:** Formal analysis, Data curation, Conceptualization. **Kedar Nath Ghimire:** Methodology, Formal analysis, Conceptualization. **Megh Raj Pokhrel:** Formal analysis, Conceptualization. **Bhoj Raj Poudel:** Supervision, Project administration, Methodology, Data curation, Conceptualization.

Declaration of competing interest

The authors declare that they have no known competing financial interests or personal relationships that could have appeared to influence the work reported in this paper.

Acknowledgements

Appendix A. Supplementary data

Supplementary data to this article can be found online at https://doi.org/10.1016/j.heliyon.2024.e37382.

References

[1] D. Bedada, K. Angassa, A. Tiruneh, H. Kloos, J. Fito, Chromium removal from tannery wastewater through activated carbon produced from Parthenium hysterophorus weed, Energy Ecol. Environ. 5 (2020) 184–195, https://doi.org/10.1007/s40974-020-00160-8.
[2] B.K. Nath, C. Chaliha, E. Kalita, Iron oxide Permeated Mesoporous rice-husk nanobiochar (IPMN) mediated removal of dissolved arsenic (As): chemometric modelling and adsorption dynamics, J. Environ. Manag. 246 (2019) 397–409, https://doi.org/10.1016/j.jenvman.2019.06.008.
[3] B.K. Biswas, J. ichi Inoue, K. Inoue, K.N. Ghimire, H. Harada, K. Ohto, H. Kawakita, Adsorptive removal of As(V) and As(III) from water by a Zr(IV)-loaded orange waste gel, J. Hazard Mater. 154 (1–3) (2008) 1066–1074, https://doi.org/10.1016/j.jhazmat.2007.11.030.
[4] R. Rai, D.R. Karki, K.P. Bhattarai, B. Pahari, N. Shrestha, S. Adhikari, S.K. Gautam, B.R. Poudel, Recent advances in biomass-based waste materials for the removal of chromium (VI) from wastewater: a review, Amrit Res J 2 (1) (2021) 37–50, https://doi.org/10.3126/arj.v2i01.40736.
[5] E. Rathore, K. Maji, K. Biswas, Nature-inspired coral-like layered [Co0.79Al0.21(OH)2(CO3)0.11]· mH2O for fast selective ppb level capture of Cr(VI) from contaminated water, Inorg. Chem. 60 (13) (2021) 10056–10063, https://doi.org/10.1021/acs.inorgchem.1c01479.
[6] B.R. Poudel, R.L. Aryal, S. Bhattarai, A.R. Koirala, S.K. Gautam, K.N. Ghimire, B. Pant, M. Park, H. Paudyal, M.R. Pokhrel, Agro-waste derived biomass impregnated with TiO_2 as a potential adsorbent for removal of as(III) from water, Catalysts 10 (10) (2020) 1–18, https://doi.org/10.3390/catal10101125.
[7] Q.L. Zhang, Y.C. Lin, X. Chen, N.Y. Gao, A method for preparing ferric activated carbon composites adsorbents to remove arsenic from drinking water, J. Hazard Mater. 148 (3) (2007) 671–678, https://doi.org/10.1016/j.jhazmat.2007.03.026.
[8] Y. Wei, S. Wei, C. Liu, T. Chen, Y. Tang, J. Ma, K. Yin, S. Luo, Efficient removal of arsenic from groundwater using iron oxide nanoneedle array-decorated biochar fibers with high Fe utilization and fast adsorption kinetics, Water Res. 167 (2019), https://doi.org/10.1016/j.watres.2019.115107.
[9] A. Chand, P. Chand, G.G. Khatri, D.R. Paudel, Enhanced removal efficiency of arsenic and copper from aqueous solution using activated Acorus calamus based adsorbent, Chem. Biochem. Eng. Q. 35 (3) (2021) 279–293, https://doi.org/10.15255/CABEQ.2021.1943.
[10] D.E. Giles, M. Mohapatra, T.B. Issa, S. Anand, P. Singh, Iron and aluminium based adsorption strategies for removing arsenic from water, J. Environ. Manag. 92 (12) (2011) 3011–3022, https://doi.org/10.1016/j.jenvman.2011.07.018.
[11] J.K. Thakur, R.K. Thakur, A.L. Ramanathan, M. Kumar, S.K. Singh, Arsenic contamination of groundwater in Nepal-An overview, Water 3 (1) (2011), https://doi.org/10.3390/w3010001.
[12] X. Yu, Y. Wei, C. Liu, J. Ma, H. Liu, S. Wei, W. Deng, J. Xiang, S. Luo, Ultrafast and deep removal of arsenic in high-concentration wastewater: a superior bulk adsorbent of porous Fe2O3 nanocubes-impregnated graphene aerogel, Chemosphere 222 (2019) 258–266, https://doi.org/10.1016/j.chemosphere.2019.01.130.
[13] D. Mohan, C.U. Pittman, Arsenic removal from water/wastewater using adsorbents-A critical review, J. Hazard Mater. 142 (1–2) (2007) 1–53, https://doi.org/10.1016/j.jhazmat.2007.01.006.
[14] M.A. Sanjrani, B. Zhou, H. Zhao, S.A. Bhutto, A.S. Muneer, S.B. Xia, Arsenic contaminated groundwater in China and its treatment options, a review, Appl. Ecol. Environ. Res. 17 (2) (2019) 1655–1683, https://doi.org/10.15666/aeer/1702_16551683.
[15] N. Bashyal, S. Aryal, R. Rai, P.C. Lohani, S.K. Gautam, M.R. Pokhrel, B.R. Poudel, Effective biosorption of phosphate from water using Fe (III)-Loaded pomegranate peel, Chem. Biochem. Eng. Q. 37 (2) (2023) 67–77, https://doi.org/10.15255/CABEQ.2022.2174.

[16] M.B. Shakoor, N.K. Niazi, I. Bibi, M. Shahid, Z.A. Saqib, M.F. Nawaz, S.M. Shaheen, H. Wang, D.C.W. Tsang, J. Bundschuh, Y.S. Ok, J. Rinklebe, Exploring the arsenic removal potential of various biosorbents from water, Environ. Int. 123 (2019) 567–579, https://doi.org/10.1016/j.envint.2018.12.049.

[17] S. Ben-Ali, Pplication of raw and modified pomegranate peel for wastewater treatment: a literature overview and analysis, Int. J. Chem. Eng. 2021 (2021), https://doi.org/10.1155/2021/8840907.

[18] Z. Yang, T. Nisar, Y. Hou, Pomegranate peel pectin can be used as an effective emulsifier, Food Hydrocoll 18 (2018) 30–35, https://doi.org/10.1016/j.foodhyd.2018.06.042.

[19] B.R. Poudel, R.L. Aryal, S.K. Gautam, K.N. Ghimire, H. Paudyal, M.R. Pokhrel, Effective remediation of arsenate from contaminated water by zirconium modified pomegranate peel as an anion exchanger, J. Environ. Chem. Eng. 9 (6) (2021), https://doi.org/10.1016/j.jece.2021.106552.

[20] X. Guo, F. Chen, Removal of arsenic by bead cellulose loaded with iron oxyhydroxide from groundwater, Environ. Sci. Technol. 39 (2005) 6808–6818, https://doi.org/10.1021/es048080k.

[21] Y. Zhang, M. Yang, X.-M. Dou, H. He, D.-S. Wang, Arsenate adsorption on an Fe−Ce bimetal oxide adsorbent: role of surface properties, Environ. Sci. Technol. 39 (2005) 7246–7253, https://doi.org/10.1021/es050775d.

[22] Z. Ren, G. Zhang, J. Paul Chen, Adsorptive removal of arsenic from water by an iron– zirconium binary oxide adsorbent, J. Colloid Interface Sci. 358 (2011) 230–237, https://doi.org/10.1016/j.jcis.2011.01.013.

[23] M.H. Salmani, M. Abedi, S.A. Mozaffari, H.A. Sadeghian, Modification of pomegranate waste with iron ions a green composite for removal of Pb from aqueous solution: equilibrium, thermodynamic and kinetic studies, Amb. Express 7 (1) (2017), https://doi.org/10.1186/s13568-017-0520-0.

[24] B.D. Pant, D. Neupane, D.R. Paudel, P. Chandra Lohani, S.K. Gautam, M.R. Pokhrel, B.R. Poudel, Efficient biosorption of hexavalent chromium from water by modified arecanut leaf sheath, Heliyon 8 (4) (2022) e09283, https://doi.org/10.1016/j.heliyon.2022.e09283.

[25] H. Paudyal, B. Pangeni, K. Inoue, H. Kawakita, K. Ohto, K.N. Ghimire, H. Harada, S. Alam, Adsorptive removal of trace concentration of fluoride ion from water by using dried orange juice residue, Chem. Eng. 223 (2013) 844–853, https://doi.org/10.1016/j.cej.2013.03.055.

[26] S. Lagergren, Zur theorie der sogenannten adsorption geloster stoffe, Kungliga svenska vetenskapsakademiens. Handlingar 24 (1898) 1–39.

[27] I. Langmuir, The adsorption of gases on plane surfaces of glass, mica and platinum, J. Am. Chem. Soc. 40 (1918) 1361–1403, https://doi.org/10.1021/ja02268a002.

[28] H.M.F. Freundlich, Uber die adsorption in losungen, J. Phys. Chem. 57 (1906) 385–470, https://doi.org/10.1515/zpch-1907-5723.

[29] K.P. Bhattarai, B.D. Pant, R. Rai, R.L. Aryal, H. Paudyal, S.K. Gautam, K.N. Ghimire, M.R. Pokhrel, B.R. Poudel, Efficient sequestration of Cr(VI) from aqueous solution using biosorbent derived from arundo donax stem, J. Chem. (2022) 2022, https://doi.org/10.1155/2022/9926391.

[30] T. Petit, L. Puskar, FTIR spectroscopy of nanodiamonds: methods and interpretation, Diam. Relat. Mater. 89 (2018) 52–66, https://doi.org/10.1016/j.diamond.2018.08.005.

[31] R.L. Aryal, A. Thapa, B.R. Poudel, M.R. Pokhrel, B. Dahal, H. Paudyal, K.N. Ghimire, Effective biosorption of arsenic from water using La(III) loaded carboxyl functionalized watermelon rind, Arab. J. Chem. 15 (2022) 3, https://doi.org/10.1016/j.arabjc.2021.103674.

[32] R. Mallampati, S. Valiyaveettil, Apple peels - a versatile biomass for water purification? ACS Appl. Mater. Interfaces 5 (10) (2013) 4443–4449, https://doi.org/10.1021/am400901e.

[33] N.M. Mahmoodi, U. Sadeghi, A. Maleki, B. Hayati, F. Najafi, Synthesis of cationic polymeric adsorbent and dye removal isotherm, kinetic and thermodynamic, J. Ind. Eng. Chem. 20 (5) (2014) 2745–2753, https://doi.org/10.1016/j.jiec.2013.11.002.

[34] S. Sert, A. Çelik, V.N. Tirtom, "Removal of arsenic(III) ions from aqueous solutions by modified hazelnut shell, Desalination Water Treat. 75 (2017) 115–123, https://doi.org/10.5004/dwt.2017.20725.

[35] S. Lou, B. Liu, Y. Qin, Y. Zeng, W. Zhang, L. Zhang, Enhanced removal of As(III) and As(V) from water by a novel zirconium-chitosan modified spherical sodium alginate composite, Int. J. Biol. Macromol. 176 (2021) 304–314, https://doi.org/10.1016/j.ijbiomac.2021.02.077.

[36] S. Ali, M. Rizwan, M.B. Shakoor, A. Jilani, R. Anjum, High sorption efficiency for As(III) and As(V) from aqueous solutions using novel almond shell biochar, Chemosphere 243 (2020), https://doi.org/10.1016/j.chemosphere.2019.125330.

[37] B.R.C. Vieira, A.M.A. Pintor, R.A.R. Boaventura, C.M.S. Botelho, S.C.R. Santos, Arsenic removal from water using iron-coated seaweeds, J. Environ. Manag. 192 (2017) 224–233, https://doi.org/10.1016/j.jenvman.2017.01.054.

[38] D. Setyono, S. Valiyaveettil, Chemically modified sawdust as renewable adsorbent for arsenic removal from water, ACS Sustain. Chem. Eng. 2 (12) (2014) 2722–2729, https://doi.org/10.1021/sc500458x.

[39] L. Hao, T. Zheng, J. Jiang, G. Zhang, P. Wang, Removal of As(III) and As(V) from water using iron doped amino functionalized sawdust: characterization, adsorptive performance and UF membrane separation, Chem. Eng. 292 (2016) 163–173, https://doi.org/10.1016/j.cej.2016.01.097.

[40] B.R. Poudel, D.S. Ale, R.L. Aryal, K.N. Ghimire, S.K. Gautam, H. Paudyal, M.R. Pokhrel, Zirconium modified pomegranate peel for efficient removal of arsenite from water, Bibechana 19 (1–2) (2022) 1–13, https://doi.org/10.3126/bibechana.v19i1-2.45943.

[41] D. Gyawali, S. Rijal, P. Basnet, K.N. Ghimire, M.R. Pokhrel, H. Paudyal, Effective biosorption of As(V) from polluted water using Fe(III)-modified Pomelo (Citrus maxima) peel: a batch, column, and thermodynamic study, Heliyon 9 (2) (2023) e13465, https://doi.org/10.1016/j.heliyon.2023.e13465.

[42] R. Rai, M. Pokharel, D. Khadka, J. Baral, D.R. Paudel, S.K. Gautam, M.R. Pokhrel, B.R. Poudel, Effective chromium (VI) removal from contaminated water by chemically modified litchi chinensis seed powder: characterization, kinetic and isotherm studies, Int. J. Environ. 12 (2) (2023) 83–102, 2023.